Stem Cell Reports, Volume *10*

Supplemental Information

Isogenic FUS-eGFP iPSC Reporter Lines Enable Quantification of FUS Stress Granule Pathology that Is Rescued by Drugs Inducing Autophagy

Lara Marrone, Ina Poser, Ian Casci, Julia Japtok, Peter Reinhardt, Antje Janosch, Cordula Andree, Hyun O. Lee, Claudia Moebius, Ellen Koerner, Lydia Reinhardt, Maria Elena Cicardi, Karl Hackmann, Barbara Klink, Angelo Poletti, Simon Alberti, Marc Bickle, Andreas Hermann, Udai Bhan Pandey, Anthony A. Hyman, and Jared L. Sterneckert

SUPPLEMENTAL FIGURES

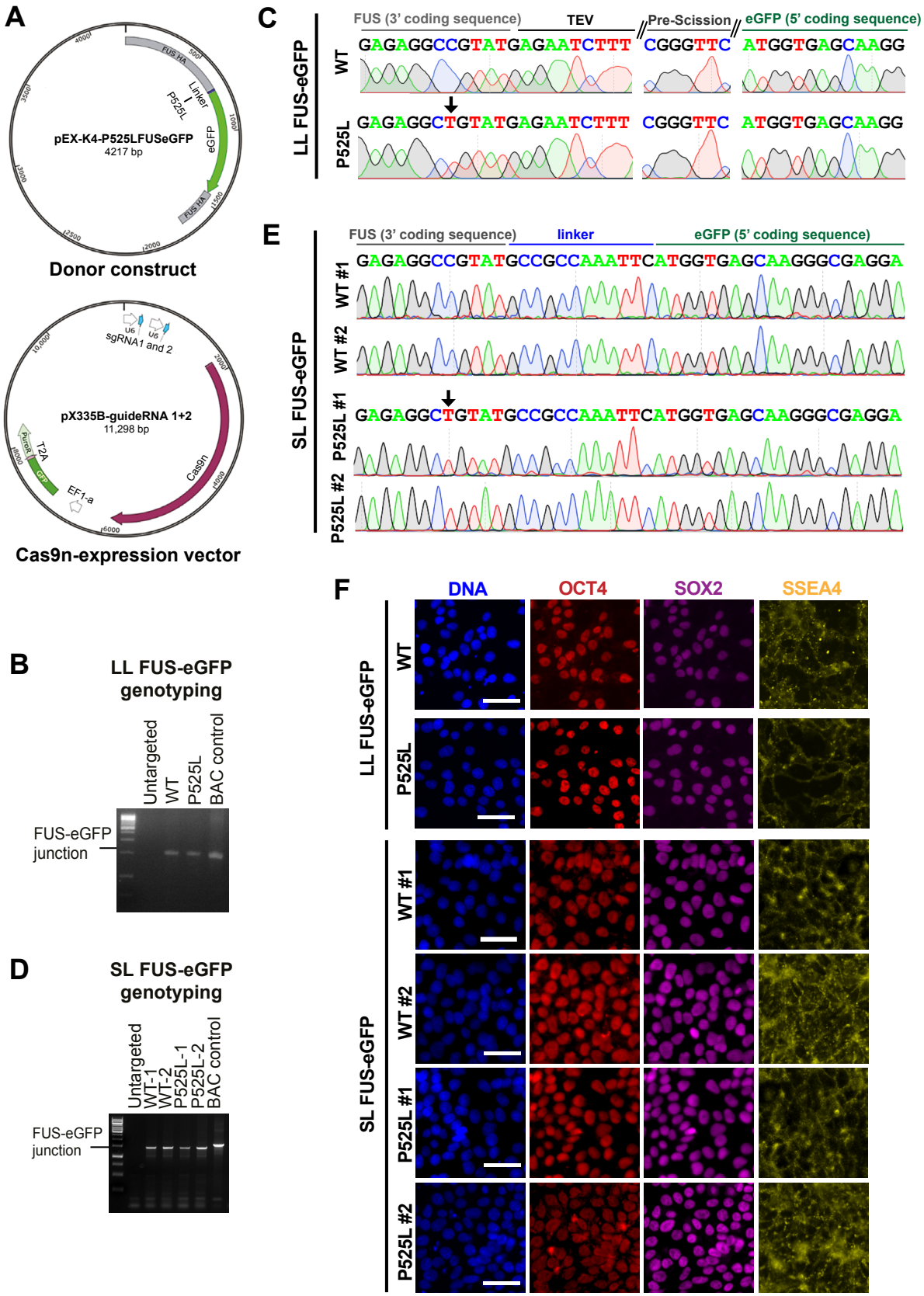

Supplemental Figure S1. Characterization of gene edited iPSCs. Related to Figure 1. (A) Schematic representation of the vectors used for gene editing: a donor construct encompassing eGFP within FUS homology arms (above); a guide-RNA expression vector encoding Cas9n (below). Genotyping PCR performed by amplifying the FUS-eGFP junction with primers indicated in Figure 1A on LL (B) and SL (D) FUS-eGFP iPSC lines. Sanger sequencing results on the PCR-amplified products confirmed in-frame fusion of eGFP within FUS c-term as well as knock-in of the P525L-coding mutation indicated by the arrow. Electropherograms are shown for both LL (C) and SL (E) FUS-eGFP iPSCs. (F) Immunostaining of gene-edited iPSCs for the indicated markers of pluripotency. Scale bar is 50 μm.

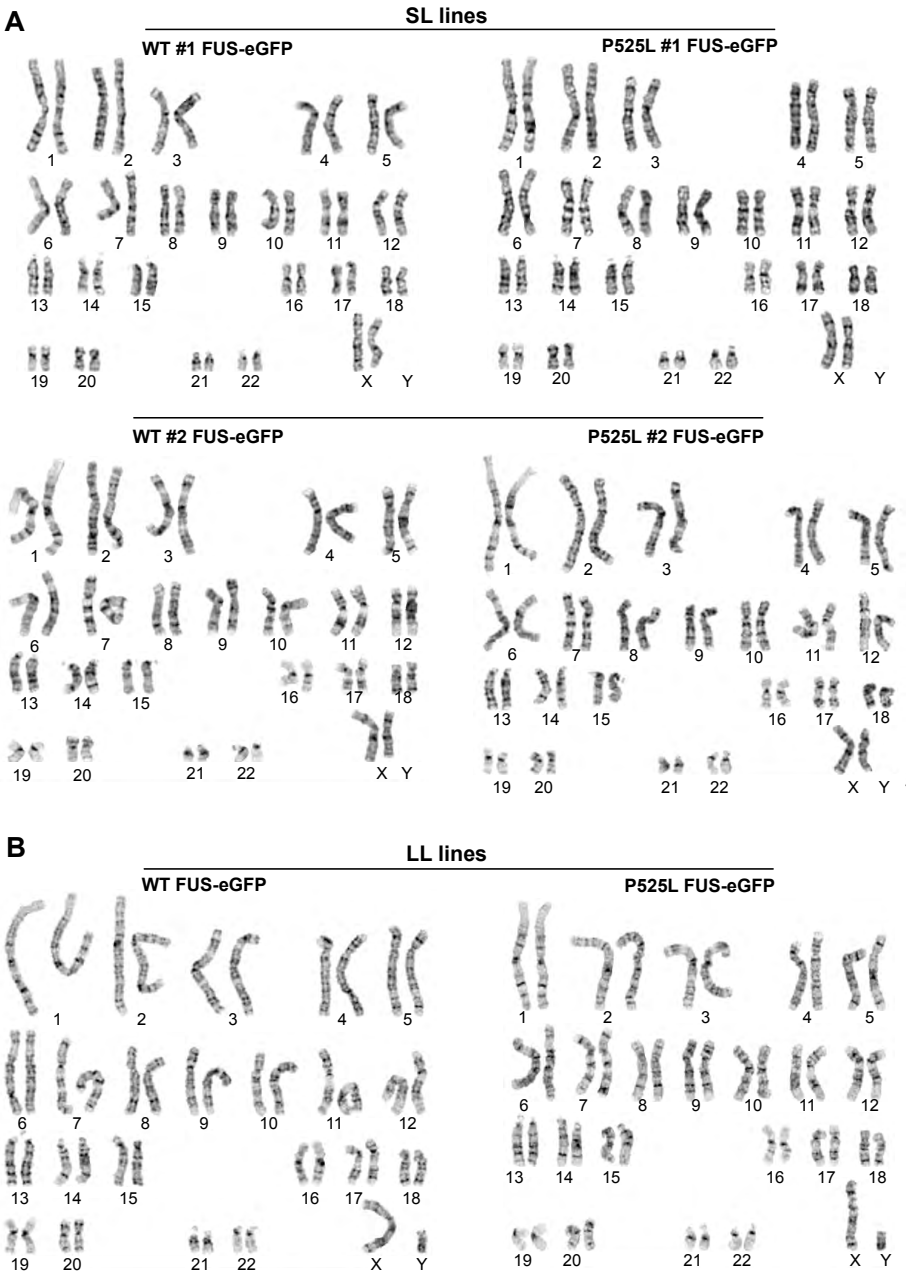

Supplemental Figure S2. Metaphase spread demonstrating euploid karyotype of the WT and P525L FUS-eGFP iPSCs used in this study. Related to Figure 1. (A) All analyzed SL iPSC lines. (B) LL iPSC lines.

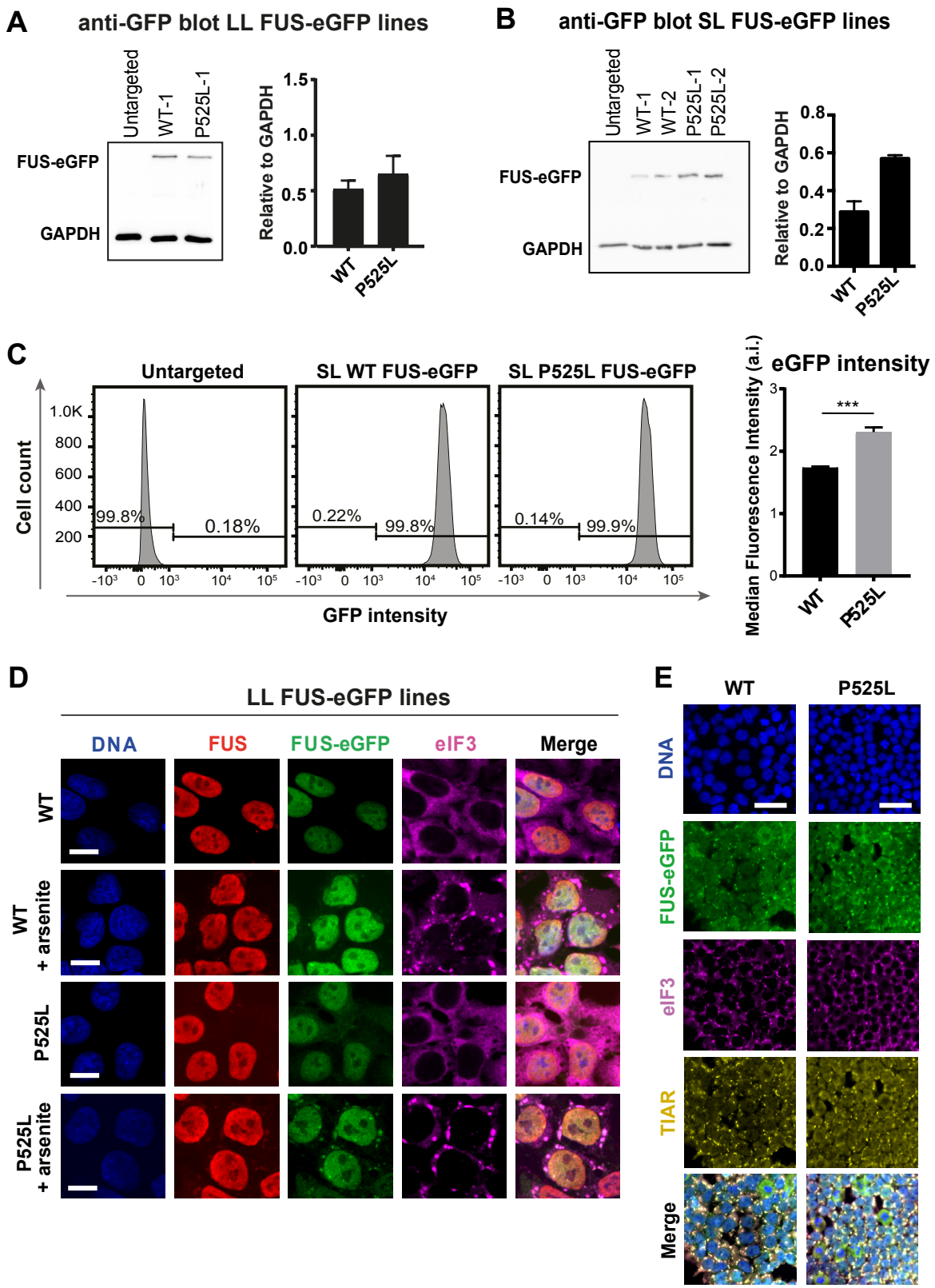

Suplemental Figure S3. Additional characterization of gene edited iPSCs. Related to Figure 1. Western blot analysis and relative quantification of FUS-eGFP fusion protein levels in LL (A) and SL (B) iPSC lines using an anti-GFP antibody. Results are shown for either one or two different WT and P525L lines as biological replicates

and were reproduced in 3 independent experiments. (C) Flow cytometry demonstrating that SL WT and P525L FUS-eGFP iPSCs homogenously express eGFP (left). Detected eGFP median fluorescence intensity is higher in P525L cells (right). Results are shown for n=3 independent experiments. (D) Conofocal micrographs showing FUS, FUS-eGFP and eIF3 subcellular localization in LL iPSC lines with or without arsenite stress. Scale bar is 10 μm. (E) Fluorescent micrographs showing co-localization of FUS-eGFP, eIF3, and TIAR in SGs of SL iPSCs. Scale bar is 10 μm.

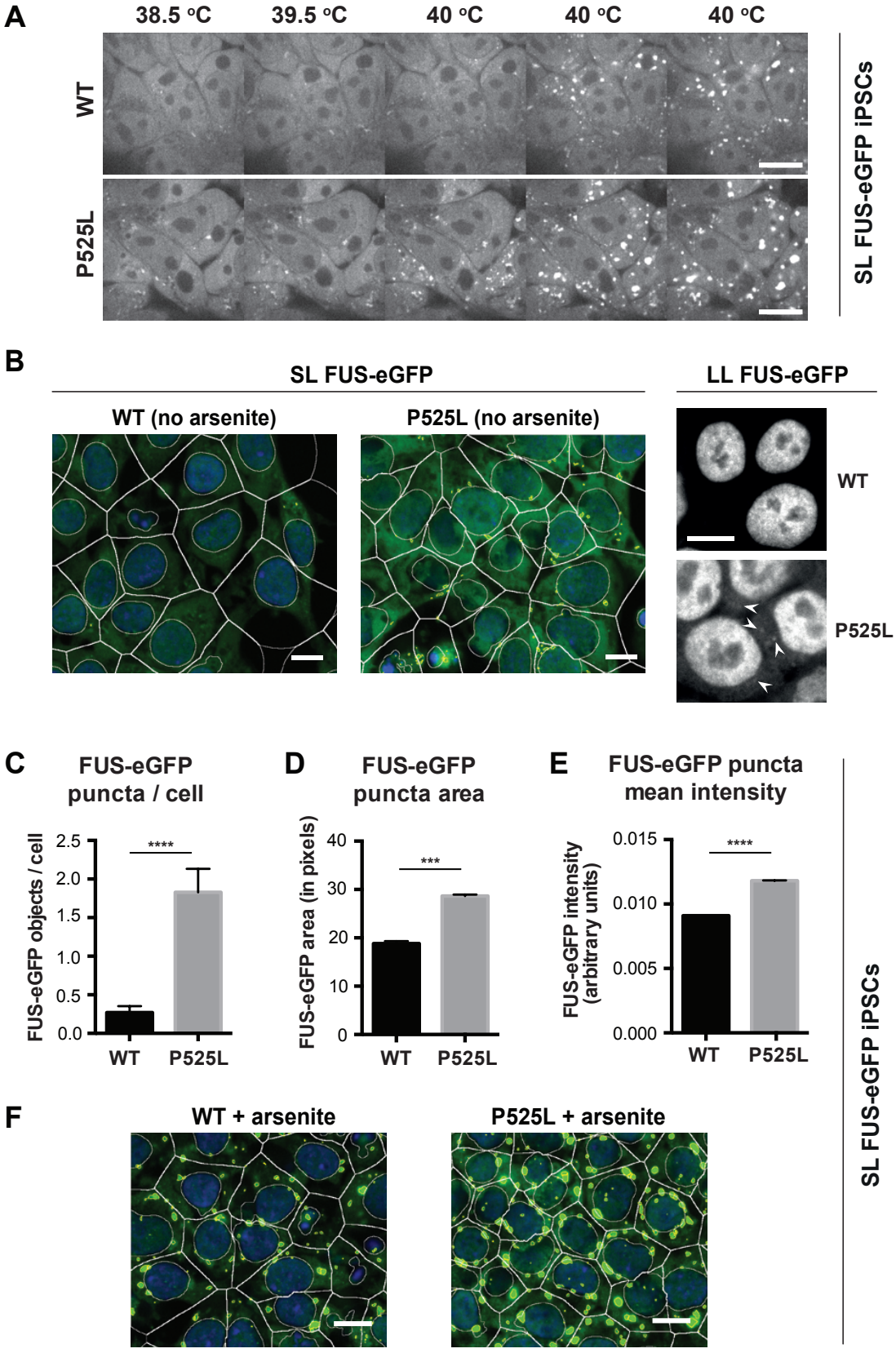
A
38.5 °C
39.5 °C
40 °C
40 °C
40 °C
WT
P525L
SL FUS-eGFP iPSCs
B
SL FUS-eGFP
LL FUS-eGFP
WT (no arsenite)
P525L (no arsenite)
WT
P525L
C
FUS-eGFP puncta / cell
FUS-eGFP objects / cell
2.5
2.0
1.5
1.0
0.5
0.0
****
WT
P525L
D
FUS-eGFP puncta area
FUS-eGFP area (in pixels)
40
30
20
10
0
***
WT
P525L
E
FUS-eGFP puncta mean intensity
FUS-eGFP intensity (arbitrary units)
0.015
0.010
0.005
0.000
****
WT
P525L
F
WT + arsenite
P525L + arsenite
SL FUS-eGFP iPSCs

Supplemental Figure S4. Characterization of FUS-eGFP stress granules and puncta. Related to Figure 2.

(A) Montage showing the reaction to heat shock of WT and P525L FUS-eGFP SL iPSCs. Individual frames and their corresponding temperature are shown from a movie taken of the indicated iPSCs undergoing heat shock. FUS-eGFP drop formation is visible. Scale bar is 10 μm. (B) Segmented confocal micrographs of unstressed iPSCs reveal the presence of FUS-eGFP puncta in both SL and LL P525L cells. Quantification of FUS-eGFP puncta per cell (C), FUS-eGFP puncta area (D), and FUS-eGFP puncta mean intensity (E) in SL iPSCs. (F) Segmented confocal micrographs of SL iPSCs treated for 1 hour with 500 μM arsenite. Scale bar is 10 μm. Images were acquired n=3 independent measurements from at least 6 positions/well per line.

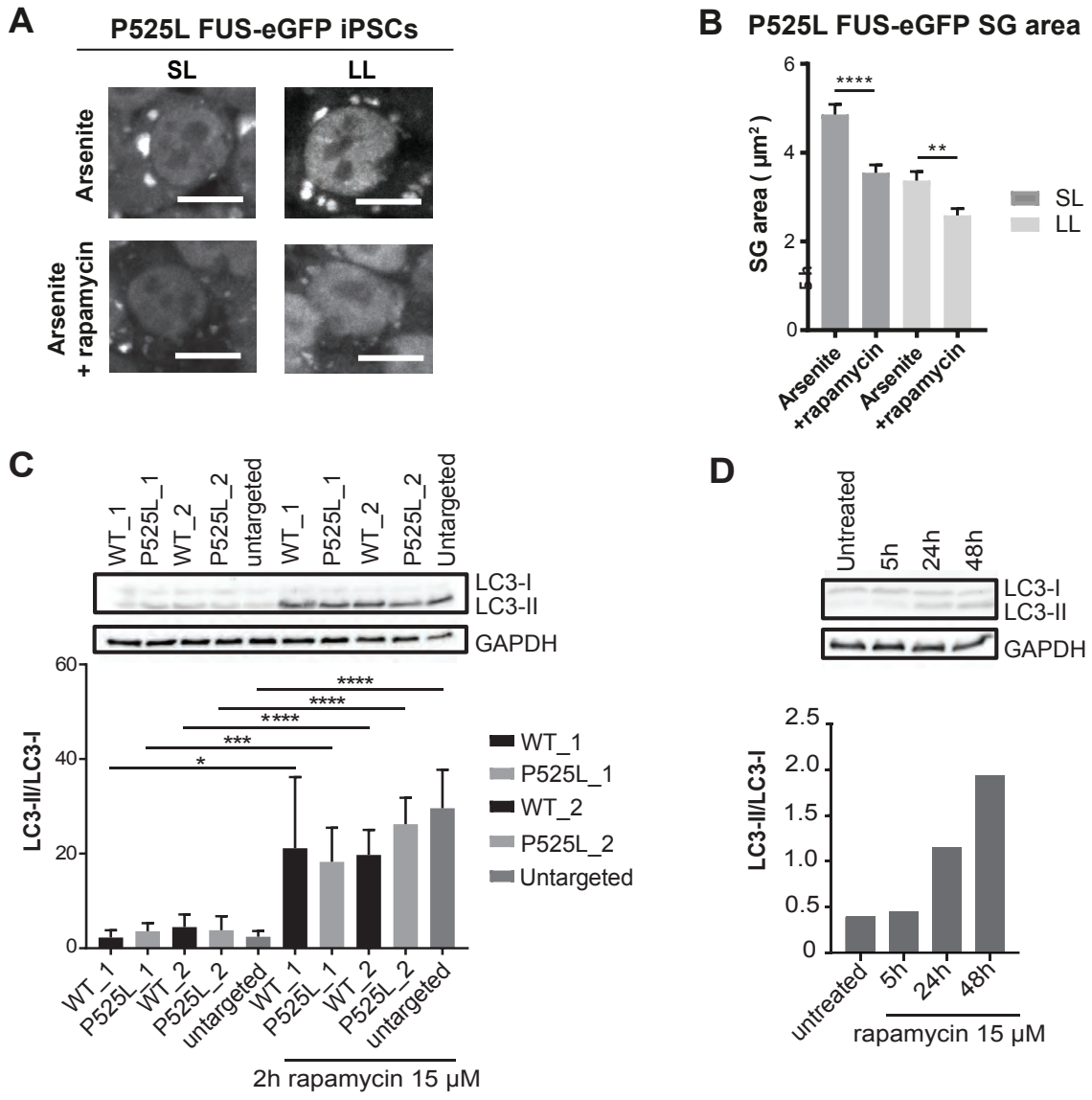

Supplemental Figure S5. Comparison of FUS SG response to rapamycin treatment in iPSCs and differentiated neurons**.** (A) Analysis of FUS stress granule (SG) characteristics with and without rapamycin treatment on P525L FUS-eGFP SL and LL iPSC lines. Rapamycin significantly reduces FUS recruitment to SGs in both lines (B). Scale bar is 10 µm. Results are shown from 3 independent measurements. (C) Western blot showing conversion of LC3-I to LC3-II upon 15 µM rapamycin treatment for 2 hours in iPSCs. Graph shows results from n=3 independent experiments. (D) Western blot demonstrating conversion of LC3-I to LC3-II in neurons upon 15 µM rapamycin treatment for the indicated time lengths.

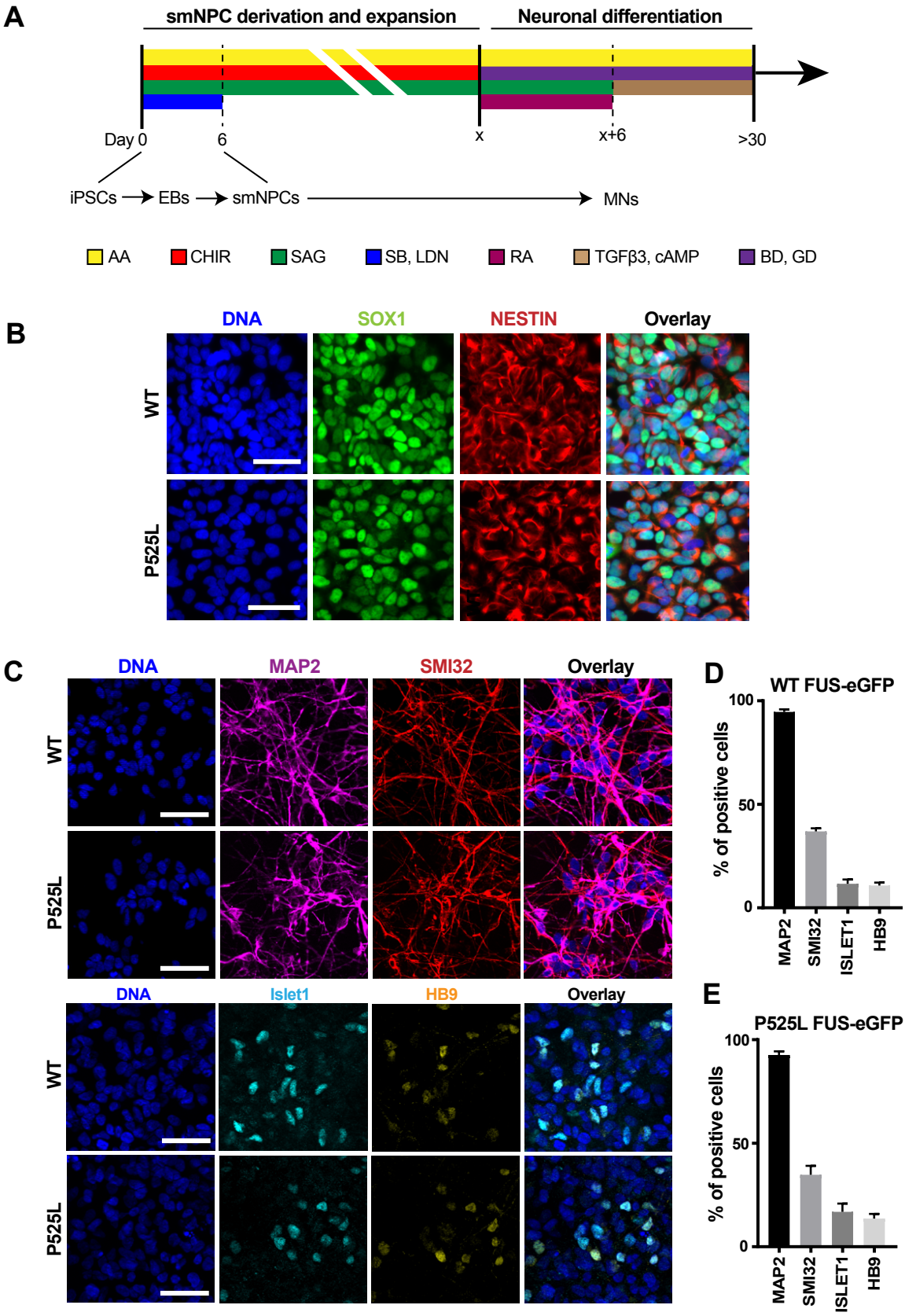

Supplemental Figure S6. Derivation of neurons from iPSCs. Related to Figure 6. (A) Diagram of differentiation protocol. AA indicates ascorbic acid; CHIR indicates CHIR99021, a GSK3 inhibitor; SAG indicates Smoothened agonist; SB indicates SB43152, an inhibitor of TGFβ receptors; LDN indicates

LDN193189, an inhibitor of BMP receptors; BD indicates BDNF; GD indicates GDNF. (B) Fluorescent micrographs of iPSC-derived smNPCs for the indicated markers. Scale bar is 50 μm. (C) Fluorescent micrographs of iPSC-derived neurons for the indicated markers. Scale bar is 50 μm. (D) Evaluation of motor neuron differentiation (MN) efficiency with the differentiation protocol described above for SL WT (D) and P525L (E) FUS-eGFP lines. Double positivity for ISLET1 and HB9 identifies bona fide MNs. Data represent results from n=3 independent measurements.

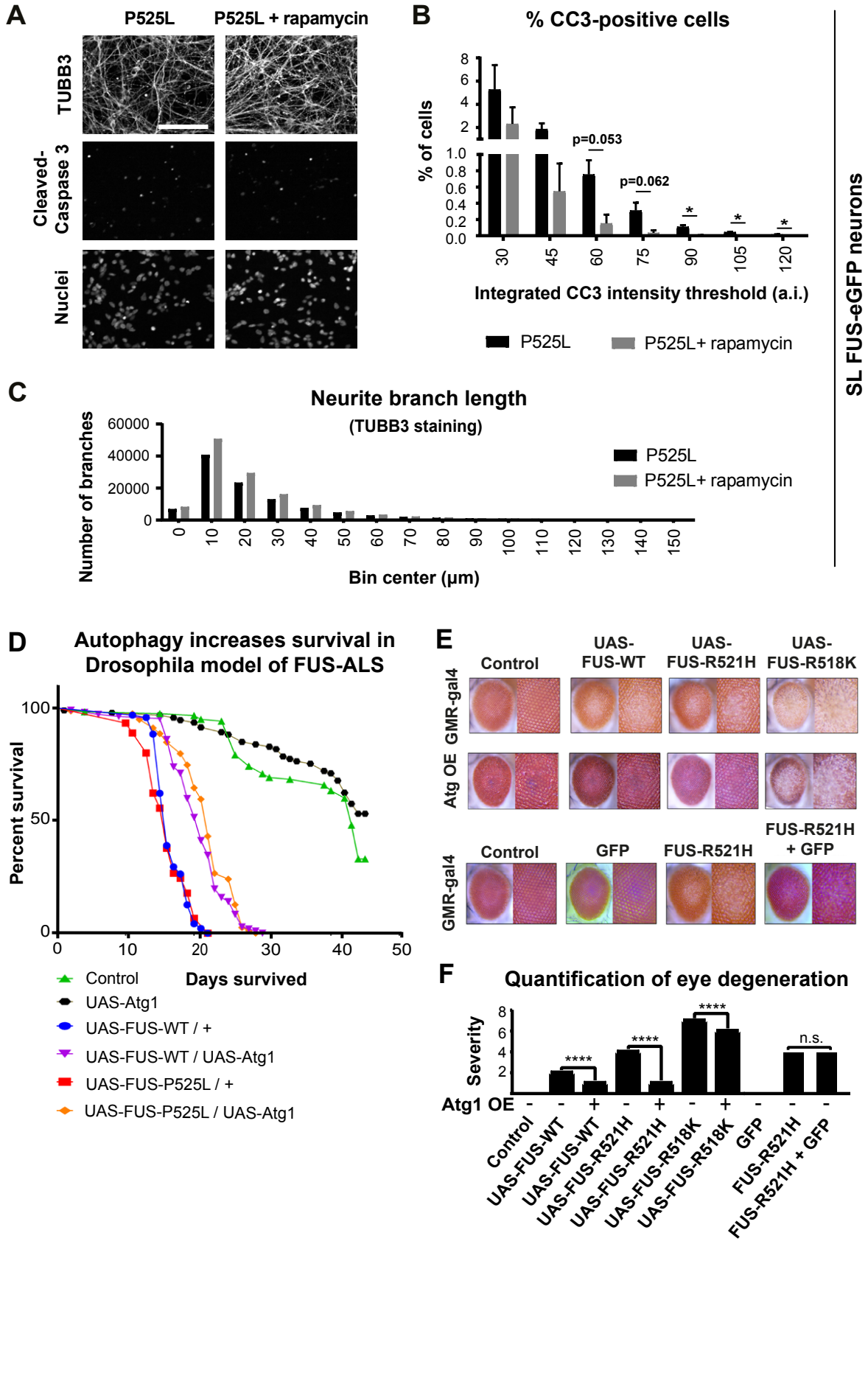
A
P525L
P525L + rapamycin
TUBB3
Cleaved-Caspase 3
Nuclei
B
% CC3-positive cells
% of cells
p=0.053
p=0.062
Integrated CC3 intensity threshold (a.i.)
P525L
P525L+ rapamycin
SL FUS-eGFP neurons
C
Neurite branch length
(TUBB3 staining)
Number of branches
Bin center (µm)
P525L
P525L+ rapamycin
D
Autophagy increases survival in Drosophila model of FUS-ALS
Percent survival
Days survived
Control
UAS-Atg1
UAS-FUS-WT / +
UAS-FUS-WT / UAS-Atg1
UAS-FUS-P525L / +
UAS-FUS-P525L / UAS-Atg1
E
Control
UAS-FUS-WT
UAS-FUS-R521H
UAS-FUS-R518K
GMR-gal4
Atg OE
Control
GFP
FUS-R521H
FUS-R521H + GFP
GMR-gal4
F
Quantification of eye degeneration
Severity
Atg1 OE
Control
UAS-FUS-WT
UAS-FUS-WT
UAS-FUS-R521H
UAS-FUS-R521H
UAS-FUS-R518K
UAS-FUS-R518K
GFP
FUS-R521H
FUS-R521H + GFP
n.s.

Supplemental Figure S7. Effect of autophagy stimulation on survival of SL neuronal cultures as well as of *in vivo* ALS models. Related to Figure 6. (A) Confocal micrographs showing tubulin and cleaved caspase 3 (CC3) staining. Scale bar is 100 μm. P525L neurons treated with rapamycin display decreased mortality calculated as percentage of CC3-positive cells, with positivity assigned according to different thresholds of CC3 signal intensity (B). Rapamycin treatment also allows the establishment of more articulated networks, as shown by a general increase in the number of shorter branch segments (C). Images were acquired from at least 6 positions/well from n=3 independent measurements per line. (D) Enhanced autophagy increases survival of Drosophila with FUS-WT and FUS-P525L. Percent survival for the indicated strains is shown over time. Neuronal ELAV-GS GAL4 driver was used to express WT or P525L FUS (designated UAS-FUS-WT and UAS-FUS-P525L, respectively) as well as ATG1 (UAS-ATG1) throughout the central nervous system. (E) Retinal degeneration in different FUS-ALS Drosophila models is suppressed by ectopic expression of Atg1, quantified in panel (F).

SUPPLEMENTAL EXPERIMENTAL PROCEDURES

CRISPR/Cas9n vectors design and generation

Synthesis of FUS-eGFP donor constructs was outsourced to Integrated DNA Technologies (IDT). Vectors consisted of the pEX-K4 plasmid backbone accommodating the eGFP-coding sequence flanked by *FUS* homology arms (ca 700 bp upstream, ca 300 bp downstream). In the P525L FUSeGFP donor construct, the WT codon (CCG) was replaced with its mutant counterpart (CTG). The guide-RNA expression vector (pX335B_hCas9_2x_long_chimeric_gRNA_G2P) was a kind gift from Dr. Boris Greber (Max Planck Institute for Molecular Biomedicine, Münster, Germany). Single-guide RNAs for gene targeting were designed using the online tool http://crispr.mit.edu/ and cloned within pX335B_hCas9_2x_long_chimeric_gRNA_G2P using BbsI and SapI restriction sites to insert the first and second guide, respectively. Each guide consisted of annealed pairs of FW and REV oligonucleotides. Specific 5'-overhanging sequences (CACC- and AAC-) were introduced in each oligo to enable successful cloning within pX335B_hCas9_2x_long_chimeric_gRNA_G2P. Ligation was performed with T4 Ligase (NEB). Obtained plasmids were used for thermal-shock transformation of competent *E. coli* TOP 10, and colony PCR was performed to assess successful cloning. Here, the FW oligonucleotide was used as forward primer and "pX335_seq_R" ("GGAAAGTCCCTATTGGCGTT") as reverse primer. The PCR product was then sequenced for quality control.

Description	5' - 3' Sequence
oligo A c-term FUS (FW)	caccGCGAGTATCTTATCTCAAGT
oligo A c-term FUS (REV)	aaacACTTGAGATAAGATACTCGC
oligo B c-term FUS (FW)	caccGTTAGGTAGGAGGGGCAGAT
oligo B c-term FUS (REV)	aacATCTGCCCCTCCTACCTAAC

iPSC culture conditions and transfection

iPSCs used in this project were previously generated and characterized (Reinhardt et al., 2013b). Cells were expanded in either mTeSR or TeSR-E8 medium (both Stem cell Technologies) at 37 ^{o}C and 5% CO_2. Medium was changed on a daily basis, and cells were regularly passaged using Accutase (Sigma) supplemented with 10 μM ROCK inhibitor Y-27632 (Abcam). For plating, cells were distributed on Matrigel (Corning)-coated plates. For CRISPR/Cas9n-mediated gene editing, 2 μg DNA (1:1 mix of donor construct and guideRNA expression

vector) were used to transfect 175,000 iPSCs with FuGENE® HD Transfection Reagent (Promega) according to manufacturer's instructions. Antibiotic selection was performed after 24 hours with 0.6 µg/ml Puromycin (Roth) overnight. After recovery, cells were seeded in clonal dilution.

Genotyping

Clones were considered for genotyping upon visible GFP expression. Medium-sized clones were partially scraped off and transferred to another plate for expansion. The remainder of each colony was lysed for genomic DNA extraction. PCR-amplification of the FUS-eGFP junction assessed successful targeting. Sequencing of the PCR-amplified products was outsourced to GATC Biotech. Allele genotyping was performed using primers flanking the eGFP sequence.

Description	5' - 3' Sequence
upstream GFP (FW)	AGCCGTTTTGTCTTTCTGAAG
within GFP_1 (REV)	CGGTGGTGCAGATGAACTT
within GFP_2 (REV)	TGCTCAGGTAGTGGTTGTCG
downstream GFP (REV)	AAACCCTTGGGTGATCAGGA

Karyotyping

Cytogenetics was performed by conventional G-banding. Cells were treated with colcemid when half confluent (0.35 µg/ml for 4 h), incubated in 75 mM KCl for 20 min at 37 °C, and fixed in freshly prepared methanol/acetic acid (3:1) at room temperature. Cell suspension was dropped onto glass slides. G-banding was performed using standard protocols (Jhanwar et al., 1994).

Quantitative RT-PCR (qRT-PCR)

Total cellular RNA was extracted from cultured cells using the RNeasy Mini Kit (Qiagen) following manufacturer's instructions. Isolated RNA was reverse-transcribed using M-MLV Reverse Transcriptase (USB Corporation) with oligo-dT_{16} primers (Metabion) for 1 h at 42 °C, followed by 10 min at 65 ^{o}C. qRT-PCR was

performed on a LightCycler LC 480 (Roche) with SYBR green PCR master mix (Life Technologies). Cycling conditions were set as follows: denaturation for 10 min at 95 ^{o}C, 40 cycles alternating 15 sec at 95 ^{o}C and 60 sec at 60 ^{o}C of 15 s. Relative expression levels were calculated using the $2^{-2\Delta}$ method, normalized to biological reference samples and using *GAPDH* as housekeeping gene.

Description	5' - 3' Sequence
FUS (FW)	CCGTGGTGGCTTCAATAAAT
FUS (REV)	GCCAGTTTCCCTGTCTGTGT
GAPDH (FW)	CTGGTAAAGTGGATATTGTTGCCAT
GAPDH (REV)	TGGAATCATATTGGAACATGTAAACC

Flow cytometric analysis

Flow cytometric data were acquired using an LSR II analyzer (BD Biosciences) and analyzed with the FlowJo software (TreeStar Inc).

Western blot analysis

Whole cell lysates were generated either in RIPA Buffer (Santa CruzBiomol) or 4 % SDS, 50 mM Tris (both Roth) supplemented with Protease inhibitor cocktail (Roche) and benzonase (Merck Millipore). 15 µg of the protein lysate were mixed with 5x Laemmli buffer and loaded on 10% or 15% SDS PAGE separation gels after incubation at 95 °C for 5 min. Blotting was performed on a PVDF membrane overnight. The membrane was blocked for 1 h in 5% milk in TBS-T 1x, and subsequently incubated with the primary antibody. After 3x washing steps with TBS-T, the membrane was incubated with HRP-coupled secondary antibodies and developed with ECL solution (GE Healthcare). Signal was detected with an image analyzer ImageQuant LAS 4000 (GE Healthcare). The following primary antibodies were used: anti-FUS antibody (AMAB90549 Sigma, 1:500), anti-GFP (sc-8334 Santa Cruz, 1:400), anti-LC3 (MBL-PM036, MBL, 1:1000), anti-GAPDH (2118S, NEB, 1:5000). Horseradish peroxidase-conjugated anti-mouse and anti-rabbit antibody (711-035-152/ 711-035-150, Dianova) were used as secondary antibodies at a dilution of 1:10,000. Acquired images were analyzed with Fiji and plotted using GraphPad Prism 7.

Neural progenitor derivation and differentiation to motor neurons

Neural progenitor cells were derived using a modified version of a previously described protocol (Reinhardt et al., 2013a). iPSCs were first converted into embryoid bodies and transferred to non-coated plates in N2B27 medium freshly supplemented with 3 µM CHIR 99021 (Axon Medchem), 10 µM SB-431542 (Abcam), 150 nM LDN-193189 (Abcam), 0.5 µM SAG (Biomol), 200 µM ascorbic acid (Sigma), and 10 µM ROCK Inhibitor (Abcam). N2B27 medium consisted of DMEM-F12/Neurobasal medium 50:50, supplemented with 0.5 % N2 supplement, 1 % B27 supplement lacking vitamin A (all Thermo Fisher Scientific), and 1 % Penicillin/Streptomycin/Glutamine (Biochrom). Cells were incubated at 37 ^{o}C, 5 % CO_2 and medium was changed every second day. On day 2, ROCK inhibitor was withdrawn. On day 6, EBs were plated on Matrigel-coated plates in smNPC expansion medium, consisting of N2B27 freshly supplemented with 3 µM CHIR 99021, 200 µM ascorbic acid and 0.5 µM SAG. Typically, cells were split 1:10 every 6 days using accutase. For motor neuron (MN) induction, smNPC expansion medium was changed to patterning medium. This consisted of N2B27 medium supplemented with 200 µM ascorbic acid, 1 µM retinoic acid (Sigma), 0.5 µM SAG, 10 ng/ml BDNF (Peprotech), 10 ng/ml GDNF (Peprotech). After 6 days, patterning medium was replaced by maturation medium (N2B27 with 5 ng/ml Activin A (eBioscience - only for the first 2 days), 1 ng/ml TGFβ3 (Peprotech), 200 µM ascorbic acid, 20 ng/ml BDNF, 20 ng/ml GDNF, 500 µM dbcAMP (Sigma). MNs were kept in culture for 3 weeks prior to downstream analysis.

Immunocytochemistry staining

For immunofluorescence, cells were fixed for 20 minutes with 4 % paraformaldehyde (EM Sciences) in PBS. Permeabilization and blocking were performed in one step using 0.1 % Triton X-100 (Sigma), 10 % FCS (GE Healthcare) and 1 % BSA in PBS (Lonza). Primary antibodies were applied overnight at 4 °C in PBS supplemented with 0.1 % BSA. Secondary antibodies were applied for 1 h at room temperature. Ultimately, cells were washed 3x, including a Hoechst (Thermo Fisher Scientific) counterstaining for nuclei in the second washing step. Primary antibodies used in this study included: goat anti-Sox2 1:200 (sc-17320, Santa Cruz), mouse anti-Oct4 1:200 (sc-5279, Santa Cruz), rabbit anti-MAP2 1:1000 (sc-20172,Santa Cruz), goat anti-eIF3 1:300 (sc-16377, Santa Cruz), mouse anti-TIAR 1:500 (610352, BD Biosciences), mouse anti-SSEA4 1:200 (MC-813-70, DSHB), goat anti-Sox1 1:400 (AF3369, R&D Systems), mouse anti-Nestin 1:500 (MAB1259 ,R&D Systems), mouse anti-SMI32 1:500 (NE1023, Millipore), rabbit anti-LC3 1:1000 (MBL-PM036, MBL).

For fluorescence microscopy analysis, secondary antibodies included goat anti-mouse AlexaFluor 647 (A-21241, Thermo), donkey anti-goat AlexaFluor 488 (A-11055, Thermo), donkey anti-rabbit AlexaFluor 568 (A-10042, Thermo), donkey anti-rabbit AlexaFluor 647 (A-31573, Thermo), donkey anti-goat AlexaFluor 568 (A-11057, Thermo), donkey anti-goat AlexaFluor 647 (A-21147, Thermo).. Cells were imaged on an inverted Apotome Zeiss Axio/Observer Z1 fluorescence microscope or a Confocal Laser Scanning Microscope 700 (Zeiss).

Stress granule induction and analysis

Cells were plated on 35 mm dishes with a glass bottom (Ibidi) and imaged with a Neo Spinning disc linked to a Clara CCD camera (Andor). Two types of cell stressors were tested: arsenite treatment and heat shock. For arsenite treatment, cells were incubated in TeSR-E8 medium supplemented with 0.5 mM Sodium Arsenite for 1 hour prior to imaging. Heat shock was performed by raising the temperature of the heating chamber (Warner) and objective heater (Bioptechs) from 37 ^{o}C to 40 ^{o}C during the imaging session. 5 positions within the dish were selected as regions of interest (ROIs) and live-imaged over time to record SG formation and development. Videos were analyzed using Fiji.

High Throughput Screening protocol

iPSCs were seeded in Greiner µClear 384-well plates at 10,000 cells/well in mTeSR medium. Compounds for screening were added on the next day at a final concentration of 10 µM. After 1 h incubation, cells were stressed with 1 µM potassium arsenite to induce stress granule formation. After 1 h of treatment, cells were fixed with 3.7% formaldehyde and stained with Hoechst and CellMaskBlue. Plates were imaged with a Yokogawa Cell Voyager CV7000 at 40x magnification. A z-stack of 5 images was acquired at 1 micron distance for the GFP channel and sum projection was carried out. IC50 of the compounds of interest was performed by testing the following concentrations: 50 µM, 25 µM, 12.5 µM, 6.25 µM, 3.13 µM, 1.56 µM, 0.78 µM 0.39 µM. The rapamycin experiment was performed at 15 µM in a time-course with the following time points: 300 min, 180 min, 120 min, 90 min, 60 min. For the experiments conducted on motor neurons, cells were seeded on Greiner 96-well plates at a density of 70,000 cells/well. After 3 weeks of maturation, rapamycin treatment was tested for the following time lengths: 30 h, 24 h, 10 h, 5h.

High content image analysis and statistics

Image analysis was carried out using CellProfiler. Briefly, nuclei were detected using Otsu's method on the Hoechst images. Cytoplasm was detected using the CellMaskBlue staining using the Nuclei as seeds. After enhancing droplets with a white top filter, stress granules were segmented according to Otsu's method. The following parameters were then extracted: number of nuclei, nuclear size and intensity; droplet number, size and intensity; average GFP signal in cytoplasm vs nucleus. Statistical analysis was carried out with KNIME. All parameters were z normalized to the mean and standard deviation of DMSO controls. Because was indicative of toxicity, compounds yielding a z-score of -2 for total number of nuclei were eliminated. Compounds with a z-score either above 3 or below -3 in any of the FUS parameters were selected, as indication of a strong effect on FUS droplet dynamics.

***Drosophila* eye degeneration experiments**

The UAS-gal4 system was utilized for targeted transgene expression in *Drosophila* eyes, under the GMR-gal4 driver. All crosses were performed at 25^{0}C. Day-1 female flies from the F1 generation were analyzed for tissue degeneration of the external eye. Severity of tissue damage was scored using a previously published scoring method that measures both the level of structural damage as well as the size of the affected area (Crippa et al., 2016; Pandey et al., 2007; Scaramuzzino et al., 2015). Statistical analyses were performed on GraphPad Prism Software. Mann-Whitney tests were performed to compare the respective FUS groups. Representative images of the left eye were captured with a Leica M205C dissection microscope with attached Leica DFC450 camera. The UAS-FUS-WT, UAS-FUS-R518K and UAS-FUS-R521H lines used in these experiments were previously described (Daigle et al., 2013; Lanson et al., 2011). The GMR-gal4 driver line and W1118 background lines are from the Bloomington *Drosophila* Stock Center (www.flystocks.bio.indiana.edu). The UAS-Atg1 overexpression line was a generous gift from Dr. Eric Baehrecke at the University of Massachusetts. attb-UAS-FLAG-eGFP (86Fb) flies were generated at BestGene, Inc. (www.thebestgene.com).

ETHICAL APPROVAL

All procedures involving human participants were performed in accordance with the ethical standards of the institutional and/or national research committee and with the 1964 Helsinki declaration and its later amendments or comparable ethical standards.

SUPPLEMENTAL REFERENCES

Crippa, V., Cicardi, M.E., Ramesh, N., Seguin, S.J., Ganassi, M., Bigi, I., Diacci, C., Zelotti, E., Baratashvili, M., Gregory, J.M., *et al.* (2016). The chaperone HSPB8 reduces the accumulation of truncated TDP-43 species in cells and protects against TDP-43-mediated toxicity. Hum Mol Genet *25*, 3908-3924.

Daigle, J.G., Lanson, N.A., Jr., Smith, R.B., Casci, I., Maltare, A., Monaghan, J., Nichols, C.D., Kryndushkin, D., Shewmaker, F., and Pandey, U.B. (2013). RNA-binding ability of FUS regulates neurodegeneration, cytoplasmic mislocalization and incorporation into stress granules associated with FUS carrying ALS-linked mutations. Hum Mol Genet *22*, 1193-1205.

Jhanwar, S.C., Chen, Q., Li, F.P., Brennan, M.F., and Woodruff, J.M. (1994). Cytogenetic analysis of soft tissue sarcomas. Recurrent chromosome abnormalities in malignant peripheral nerve sheath tumors (MPNST). Cancer Genet Cytogenet *78*, 138-144.

Lanson, N.A., Jr., Maltare, A., King, H., Smith, R., Kim, J.H., Taylor, J.P., Lloyd, T.E., and Pandey, U.B. (2011). A Drosophila model of FUS-related neurodegeneration reveals genetic interaction between FUS and TDP-43. Hum Mol Genet *20*, 2510-2523.

Pandey, U.B., Nie, Z., Batlevi, Y., McCray, B.A., Ritson, G.P., Nedelsky, N.B., Schwartz, S.L., DiProspero, N.A., Knight, M.A., Schuldiner, O., *et al.* (2007). HDAC6 rescues neurodegeneration and provides an essential link between autophagy and the UPS. Nature *447*, 859-863.

Reinhardt, P., Glatza, M., Hemmer, K., Tsytsyura, Y., Thiel, C.S., Hoing, S., Moritz, S., Parga, J.A., Wagner, L., Bruder, J.M., *et al.* (2013a). Derivation and Expansion Using Only Small Molecules of Human Neural Progenitors for Neurodegenerative Disease Modeling. PLoS One *8*, e59252.

Reinhardt, P., Schmid, B., Burbulla, L.F., Schondorf, D.C., Wagner, L., Glatza, M., Hoing, S., Hargus, G., Heck, S.A., Dhingra, A., *et al.* (2013b). Genetic correction of a LRRK2 mutation in human iPSCs links parkinsonian neurodegeneration to ERK-dependent changes in gene expression. Cell Stem Cell *12*, 354-367.

Scaramuzzino, C., Casci, I., Parodi, S., Lievens, P.M., Polanco, M.J., Milioto, C., Chivet, M., Monaghan, J., Mishra, A., Badders, N., *et al.* (2015). Protein arginine methyltransferase 6 enhances polyglutamine-expanded androgen receptor function and toxicity in spinal and bulbar muscular atrophy. Neuron *85*, 88-100.